N95-11020

THREE-DIMENSIONAL MODELLING OF TRACE SPECIES IN THE ARCTIC LOWER STRATOSPHERE

Martyn Chipperfield Daniel Cariolle and Pascal Simon
Centre National de Recherches Météorologiques, 42 Ave. Coriolis, 31057 Toulouse, France

Richard Ramaroson
Office National d'Etudes et de Recherches Aérospatiales, 92322 Châtillon, France

ABSTRACT

A three-dimensional radiative-dynamical-chemical model has been developed and used to study some aspects of modelling the polar lower stratosphere. The model includes a comprehensive gas-phase chemistry scheme as well as a treatment of heterogeneous reactions occurring on the surface of polar stratospheric clouds. Tracer transport is treated by an accurate, non-dispersive scheme with little diffusion suited to the representation of strong gradients. Results from a model simulation of early February 1990 are presented and used to illustrate the importance of the model transport scheme. The model simulation is also used to examine the potential for Arctic ozone destruction and the relative contributions of the chemical cycles responsible.

INTRODUCTION

We present results from a 3D model which has been developed for the study of trace gases in the polar lower stratosphere. A detailed account of the model is given in a paper in preparation (Chipperfield et al 1993) which describes a series of experiments in the 1989-90 Arctic winter including a comparison with the available measurements. In this short article we concentrate on illustrating the improved model performance on changing from a spectral transport scheme to the second order moments scheme of Prather (1986) and also on the efficiency of various catalytic ozone destruction cycles in the polar lower stratosphere.

The northern winter of 1989-90 was extremely cold with temperatures in the polar lower stratosphere below the seasonal average (e.g. see Naujokat et al 1990). An inspection of the ECMWF (European Centre for Medium-Range Weather Forecasts) analyses for this winter shows that type I (nitric acid trihydrate) PSC's could have formed from mid December to early February at which time a stratospheric warming occurred (although the vortex did not break down). Temperatures in late January and early February were cold enough to permit the formation of type II (ice) PSC's. The persistence of cold temperatures into February would have provided the greatest opportunity of PSC-processed air to experience sunlight, especially as during this period the cold vortex was displaced from the pole towards northern Scandinavia.

THE MODEL

We have used a middle atmosphere general circulation model (GCM) to generate wind fields which are used in a chemical transport model (CTM). The GCM used is the tropospheric-stratospheric version of the 'Emeraude' spectral model described by Cariolle et al (1990). The model has 30 levels (with a resolution of about 1.8km in the lower stratosphere) and, for the experiments presented here, has been employed in the horizontal truncation of T21 (corresponding to a gaussian grid of 5.6° x 5.6°). The CTM uses the same grid as the GCM and advects the tracers using the scheme of Prather (1986) which conserves the second order moments of the tracer distribution. The chemical species are transported using this scheme rather than the spectral scheme of the GCM as it is less diffusive and better at representing the strong gradients often found in chemical species concentrations, for instance at the vortex boundary (see below). The CTM contains 20 integrated chemical species (O_3, O, H_2O_2, NO, NO_2, NO_3, N_2O_5, HNO_3, HO_2NO_2, Cl, ClO, $ClONO_2$, HOCl, HCl, OClO, Cl_2O_2, Br, BrO, $BrONO_2$, BrCl) and 3 which are assumed to be in photochemical equilibrium (H, OH, HO_2). Photochemical data is taken from NASA/JPL (1990). The chemical integration is performed using the semi-implicit symmetric scheme of Ramaroson et al (1992). Fixed zonal mean fields of CH_4 and CO (taken from a 2D model) are used for reactions such as $Cl + CH_4 \rightarrow HCl + CH_3$. The model temperature, water vapour and nitric acid fields are used to predict the occurrence of type I (Hanson and Mauersberger 1988) and type II PSC's (Murray 1967). When such PSC's occur the following five heterogeneous reactions are activated:

$$N_2O_5(g) + H_2O(s) \rightarrow 2HNO_3(s)$$
$$N_2O_5(g) + HCl(s) \rightarrow ClNO_2(g) + HNO_3(s)$$
$$ClONO_2(g) + H_2O(s) \rightarrow HOCl(g) + HNO_3(s)$$
$$ClONO_2(g) + HCl(s) \rightarrow Cl_2(g) + HNO_3(s)$$

C-2

$$HOCl(g) + HCl(s) \rightarrow Cl_2(g) + HNO_3(s)$$

The rates of these heterogeneous reactions are calculated using reaction probabilities from experimental data (see WMO/UNEP 1991 for discussion and recommended values).

INITIALISATION

The GCM is initialised with meteorological data from the ECMWF below 10hPa and from climatology above. The O_3 field was generated from TOMS data using the method described by Riishojgaard et al (1992). The other chemical species were initialised using data from a 2D model. Polewards of 30°N, between 200hPa and 10hPa, the longer-lived chemical species were initialised with the 2D data transformed into the coordinates of potential vorticity (PV) and potential temperature (θ) in order to capture the azonal nature of the polar vortex.

RESULTS

To illustrate some aspects of the model performance we present results from four 10 day simulations of the CTM which start on the 4th February 1990. During this period temperatures in the polar vortex were cold enough to allow the formation of both type I and type II PSC's and the vortex itself was displaced towards Scandinavia (figure 1). The winds for the CTM were obtained from a 10 day run of the GCM starting from the same date. The low resolution (T21) of the GCM run means that after a few days the meteorological forecast of the model is degraded. Run A of the CTM contained only gas-phase chemistry while run B included the treatment of heterogeneous reactions described above. To compare the effect of two transport schemes we performed two further runs (C and D) of the CTM (equivalent to runs A and B respectively) using the spectral scheme (as employed in the GCM) for tracer advection. In runs C and D negative mixing ratios caused by the transport scheme were corrected by redistributing the negative mass amongst other members of the same chemical family within a model box.

Chlorine Processing

Figure 2a shows the difference in HCl mixing ratio on the 500K isentropic surface between run B and run A after 10 days of model integration. Air within the polar vortex (indicated by the PV map in figure 3) has been processed by the localised region of PSC's over northern Scandinavia in run B, converting virtually all of the HCl (2ppbv) at this altitude to active chlorine (the initial conditions assumed that the chlorine species were partitioned purely on the basis of gas-phase chemistry). Note the sharp gradients in HCl at the edge of the PSC-processed region in figure 2a. The non-diffusive nature of the Prather transport scheme performs well in maintaining these strong gradients. Figure 2b shows the difference in mixing ratio for $ClONO_2$. At the centre of the vortex is a minimum surrounded by a ring of high $ClONO_2$. In calculating the rates of chemical reactions the model simply uses the average concentration of each tracer within a box, which therefore assumes rapid, complete mixing within that box. Therefore in run B the rate of production of $ClONO_2$ is probably overestimated. To illustrate the improvement of this transport scheme over the spectral scheme, as employed in the GCM, figure 4a is the same as figure 2a but for runs C and D. Although the processing of HCl in the vortex is similar the gradients at the edge of the vortex are smoothed out and, more unrealistically, the HCl-poor air is 'transported' to mid-latitudes. The limitations of the spectral scheme, in the comparatively low resolution of T21, are more apparent with $ClONO_2$. Figure 4b shows much larger mixing ratios of $ClONO_2$ than figure 2b both inside and outside the polar vortex. A local minimum in the difference is coincident with the region of PSC's at 80°N, 90°E. Chlorine nitrate

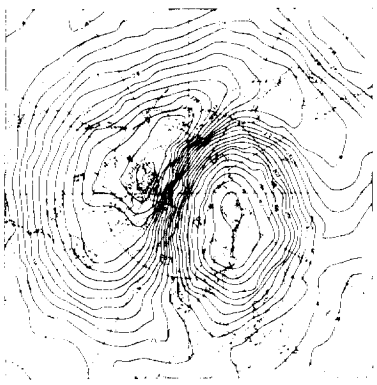

Fig. 1. Temperature (K) at 50hPa on the 6th February 1990 from the T21 GCM simulation (initialised on February 4th) used to produce the wind fields for the CTM. At this altitude type I PSC's could form at 195K and type II PSC's at 190K. Contour interval 2K.

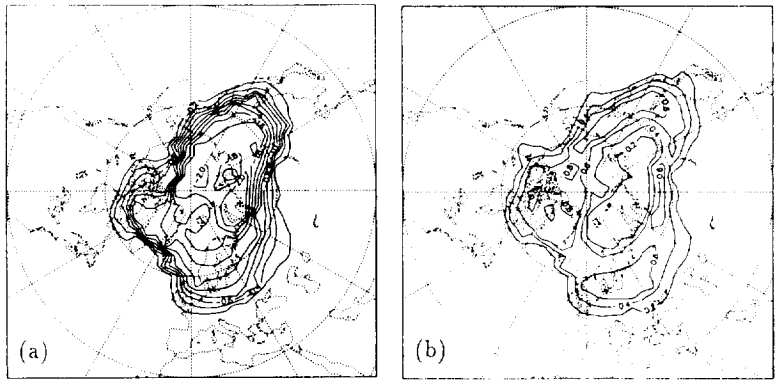

Fig. 2. Difference in a) HCl and b) $ClONO_2$ mixing ratio (ppbv) between run B and run A on the 500K surface on 14th February. Contour interval 0.2ppbv.

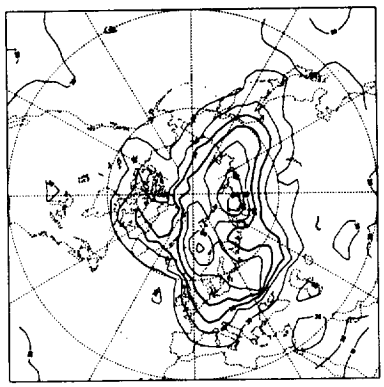

Fig. 3. Potential vorticity ($x10^6$ $Km^2s^{-1}kg^{-1}$) on the 500K surface on 14th February 1990 from the GCM model simulation. Contour interval $10x10^6$.

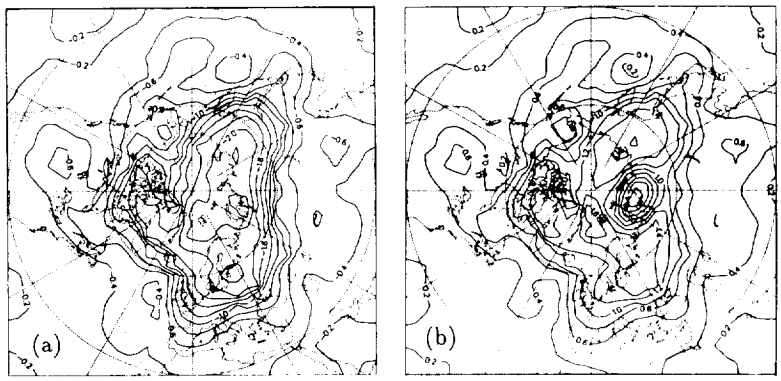

Fig. 4. Difference in a) HCl and b) $ClONO_2$ mixing ratio (ppbv) between run D and run C on the 500K surface on 14th February. Contour interval 0.2ppbv.

is produced by reaction of ClO (typically high inside the vortex) with NO_2 (typically high at mid-latitudes). Figure 4b shows the dangers of the spectral transport schemes where diffusion, due to the Gibb's effect, 'transports' ClO to mid-latitudes and NO_2 into the polar vortex resulting in the formation of large amounts of $ClONO_2$. The properties of various transport schemes have been well investigated in several 1D passive tracer experiments (e.g. Müller 1992 and references therein). However, the examples above show that when chemical interactions between tracers are considered the problems are compounded and results from a diffusive scheme, such as the spectral one employed here, rapidly become unrealistic. The performance of the spectral scheme could be improved by the use of a more sophisticated filter to remove the Gibb's fringes, or by increasing the resolution.

Ozone budget

The processing of air by PSC's in run B leads to elevated levels of ClO and BrO in the polar vortex. Figure 5a is a latitude height cross section of ClO at 33°E at 12H GMT on February 6th. A peak mixing ratio of 1.0ppbv of ClO is located at 30hPa between 55°N and 70°N. The altitude distribution of the ClO is determined by the upper limit of PSC's in the model (around 20hPa) and the abundance of inorganic chlorine at lower altitudes. In the Arctic, climatology shows that PSC's tend to occur at higher altitudes than in the Antarctic. The peak mixing ratio of BrO (figure 5b) is 8pptv at a similar altitude and between 50°N and 65°N. The subsequent destruction of ozone in the model has been analysed for the following 3 cycles, which dominate the ozone loss in the polar lower stratosphere:

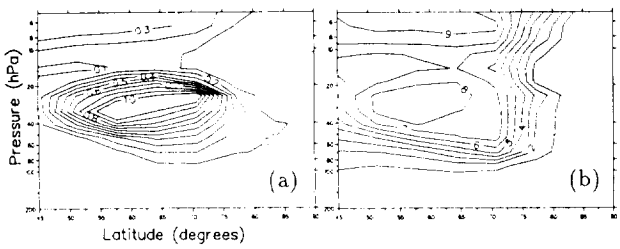

Fig. 5. Mixing ratio of a) ClO (ppbv) and b) BrO (pptv) at 33°E on 6th February at 12H GMT from run B.

$$\text{I}\quad \begin{aligned} ClO + ClO + M &\rightarrow Cl_2O_2 + M \\ Cl_2O_2 + h\nu &\rightarrow ClO_2 + Cl \\ ClO_2 + M &\rightarrow Cl + O_2 + M \\ 2(Cl + O_3 &\rightarrow ClO + O_2) \\ \text{net} : 2O_3 &\rightarrow 3O_2 \end{aligned}$$

$$\text{II}\quad \begin{aligned} ClO + BrO &\rightarrow Cl + Br + O_2 \\ Cl + O_3 &\rightarrow ClO + O_2 \\ Br + O_3 &\rightarrow BrO + O_2 \\ \text{net} : 2O_3 &\rightarrow 3O_2 \end{aligned}$$

$$\text{III}\quad \begin{aligned} ClO + O &\rightarrow Cl + O_2 \\ Cl + O_3 &\rightarrow ClO + O_2 \\ \text{net} : O + O_3 &\rightarrow 2O_2 \end{aligned}$$

Cycle II could also be initialised by the formation and subsequent photolysis of BrCl. The instantaneous rate of ozone loss due to these 3 cycles is shown in figure 6. The efficiency of these cycles depends strongly on altitude and also on the latitude. Destruction due to cycle I (figure 6a) peaks at over 25ppbv/day at 40hPa, 60°N. The efficiency of this cycle is greater at lower altitudes due to the 3 body formation of Cl_2O_2. The low abundance of ClO below 50hPa, however, limits ozone destruction due to this cycle below this height. Loss due to cycle II is similar to that due to cycle I and shows a maximum of over 20ppbv/day at around 40hPa. Ozone loss at lower altitudes would have a larger effect on the integrated column but on the model

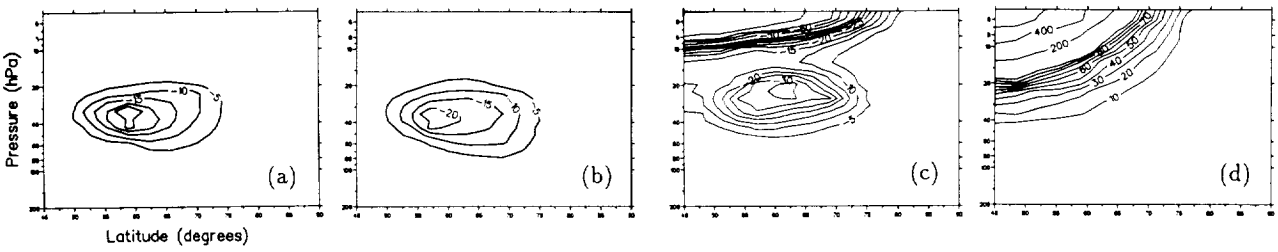

Fig. 6. Ozone loss (ppbv/day) due to a) cycle I b) cycle II c) cycle III and d) production due to photolysis of O_2 at 33°E on 6th February at 12H GMT from run B (note irregular contour spacing in figures 6c and 6d).

day shown the catalytic cycle with the largest rate of ozone mixing ratio loss is cycle III. Between 20-30hPa loss due to this cycle is over 35ppbv/day. The efficiency of cycle III increases with height as the concentration of atomic oxygen increases and in figure 6 it is the dominant loss mechanism above 30hPa (in the trajectory model study of McConnell et al (1991) cycle III was the major loss cycle above 19km). To some extent loss due to cycle III at around 20hPa is offset by in-situ production of odd oxygen by the photolysis of O_2 (figure 6d) which increases rapidly at higher altitudes and lower latitudes. At 20hPa, 60°N the rate of production is 50ppbv/day. An estimate of the total loss of ozone during the winter period would need to take to account of the efficiency of these catalytic cycles as a function of time and location. This is discussed in more detail in Chipperfield et al (1993).

SUMMARY

These results highlight the importance of a non-diffusive transport scheme in 3D chemical model studies of the polar stratosphere. The expense of 3D chemical calculations means that comparatively low resolutions (such as T21) are usually employed. Such low resolutions provide a stern test for the transport scheme employed especially when chemical interactions between species are considered. In our experiments the Prather (1986) transport scheme performs significantly better than a spectral scheme. The performance of the Prather scheme itself could be improved by taking account of the species distribution within a box in the calculation of chemical rates. The chemical cycles controlling the destruction of ozone in the Arctic lower stratosphere vary strongly with altitude. The rate of ozone loss due to cycles involving ClO + BrO can be significant compared to loss due to ClO + ClO. When PSC processing leads to elevated ClO at altitudes above about 30hPa the destruction cycle involving ClO + O becomes efficient.

Acknowledgements. MPC thanks The Royal Society and NATO for a scientific fellowship.

REFERENCES

Cariolle, D., A. Lasserre-Bigorry, J.F. Royer and J.F. Geleyn, A general circulation model simulation of the springtime antarctic ozone decrease and its impact on mid-latitudes, J. Geophys. Res., 95, 1883-1898, 1990.

Chipperfield, M.P., R. Ramaroson, D. Cariolle, P. Simon and D.J. Lary, Three-dimensional modelling of trace gases in the Arctic lower stratosphere during winter 1989-90, J. Geophys. Res., (submitted), 1993.

Hanson, D., and K. Mauersberger, Laboratory studies of the nitric acid trihydrate: implications for the south polar stratosphere, Geophys. Res. Lett., 15, 855-858, 1988.

McConnell, J.C., W.F.J. Evans and E.M.J. Templeton, Model simulation of chemical depletion of Arctic ozone during the winter of 1989, J. Geophys. Res., 96, 10923-10930, 1991.

Müller, R., The performance of classical versus modern finite-volume advection schemes for atmospheric modelling in a one-dimensional test-bed., Mon. Wea. Rev., 120, 1407-1415, 1992.

Murray, F.W., On the computation of saturation vapour pressure, J. Appl. Met., 6, 203-204, 1967.

NASA/JPL, W.B. DeMore et al, Chemical kinetics and photochemical data for use in stratospheric modelling, Evaluation no. 9, JPL publication 90-1, 1990.

Naujokat, B., et al., The stratospheric winter of 1989/90: very cold with a pronounced minor warming and a late final warming, Beilage zur Berliner wetterkarte, 75/90, SO12/90, 1990.

Prather, M.J., Numerical advection by conservation of second order moments, J. Geophys. Res., 91, 6671-6681, 1986.

Ramaroson, R., M. Pirre and D. Cariolle, A box model for on-line computations of diurnal variations in a 1D model: Potential for application to multidimensional cases, Ann. Geophysicae, 10, 416-428, 1992.

Riishojgaard, L.P., F. Lefevre, D. Cariolle, P. Simon, A GCM simulation of the Northern hemisphere ozone field in early February 1990 using satellite total ozone for model initialisation, Ann. Geophysicae, 10, 54-74, 1992.

WMO/UNEP, Scientific assessment of ozone depletion, Report No. 25, 1991.